Appl. Math. Mech. -Engl. Ed., **33**(5), 649–662 (2012)
DOI 10.1007/s10483-012-1577-8

Applied Mathematics and Mechanics (English Edition)

Numerical study of flow and heat transfer during oscillatory blood flow in diseased arteries in presence of magnetic fields*

A. SINHA[1], J. C. MISRA[2]

(1. School of Medical Science and Technology, Indian Institute of Technology, Kharagpur 721302, India;
2. Department of Mathematics, Institute of Technical Education and Research, Siksha O Anusandhan University, Bhubaneswar 751030, India)

Abstract A problem motivated by the investigation of the heat and mass transfer in the unsteady magnetohydrodynamic (MHD) flow of blood through a vessel is solved numerically when the lumen of the vessel has turned into the porous structure. The time-dependent permeability and the oscillatory suction velocity are considered. The computational results are presented graphically for the velocity, the temperature, and the concentration fields for various values of skin friction coefficients, Nusselt numbers, and Sherwood numbers. The study reveals that the flow is appreciably influenced by the presence of a magnetic field and also by the value of the Grashof number.

Key words mass transfer, radiation, suction velocity, skin-friction

Chinese Library Classification O357
2010 Mathematics Subject Classification 74F05

Nomenclature

u,	dimensionless velocity;	C_∞,	concentration of the ambient fluid;
g,	acceleration due to gravity;	D,	thermal molecular diffusivity;
β,	coefficient of thermal expansion;	ϵ,	small positive constant ($\ll 1$);
β^*,	coefficient of thermal expansion with concentration;	q_{r},	radiative heat flux;
		c_p,	specific heat at constant pressure;
B_0,	applied magnetic field;	σ^*,	Stefan-Boltzmann constant;
v_0,	scale of suction velocity (non-zero constant);	k^*,	mean absorption coefficient;
		k_1,	thermal conductivity;
ν,	kinematic coefficient of viscosity;	K_0,	constant permeability of the medium;
σ,	electrical conductivity;	n',	frequency of oscillation;
ρ,	density of fluid;	M,	Hartmann number;
T,	temperature;	Gr,	Grashof number;
C,	concentration;	Gm,	solute Grashof number;
T_{w},	surface temperature;	Pr,	Prandtl number;
C_{w},	concentration of fluid at the sheet;	Nr,	radiation parameter;
T_∞,	temperature of the ambient fluid;	Sc,	Schmidt number.

* Received Mar. 9, 2011 / Revised Nov. 12, 2011
Corresponding author J. C. MISRA, Professor, Ph. D., E-mail: misrajc@gmail.com

1 Introduction

Flow of blood through arteries is an important physiological problem, and is of considerable interest for biomedical researchers, physiologists, and clinicians. One of the important aspects of this problem that requires special attention is the deviation in the flow characteristics of blood when the artery is exposed to an externally applied magnetic field, which has been the subject of vigorous researches in recent years. Various important aspects of blood flow in arteries and capillaries have been studied quite extensively by Misra and his co-workers[1–13]. Very recently, the electro-osmotic flow of blood was investigated by Misra et al.[14]. When the human body is subjected to a vibration environment, the flow behaviour of blood also suffers from the considerable changes both qualitatively and quantitatively. Although human body has remarkable adaptability to changes, there can be oscillatory flow of blood due to the prolonged exposure of the body to vibration. This may lead to many health problems, like headache, abdominal pain, losing vision, venous pooling of blood in the extremities, and increased pulse rate on account of disturbances in blood flow. The human body is also quite often subjected to acceleration. As we know, in many situations, like travelling, driving, jogging, and using lathe machines, the human body is subjected to vibrations (body acceleration). For athelets, vibration occurs quite frequently due to their sudden movement. Several successful attempts have been made recently by Misra and Chakravarty[15] and Misra and Singh[16] towards the mathematical modelling of different vascular components of the body subjected to vibration excitation and other types of forces experienced by these components in the normal physiological state.

Several studies on the magnetohydrodynamic (MHD) effects on blood flow and some other related problems were performed by some investigators[17–20] when the flow takes place through porous media. Vardanyan[21] explored the potential use of MHD principles in prevention and rational therapies of arterial hypertension. According to the investigation reported by Barnothy[22], the heat rate decreases when a biological system is exposed to an external magnetic field. The electrocardiographic (ECG) pattern taken in the presence of a magnetic field can not only provide information on blood flow, but also offer a new non-invasive method for studying the cardiac performance.

In case of some arterial diseases, e.g., in the lumen of an artery, a porous structure is formed by fatty substances, cholesterol, and blood clots. Coronary arteries are more prone to such pathological states[23]. In such an arterial segment, blood has to flow through a porous structure[24]. Several researchers[25–26] have studied some problems of free convection and mass transfer in the flow of a viscous fluid through a porous medium. In these studies, the permeability of the porous medium is assumed to be constant. However, a porous material containing the fluid is a non-homogeneous medium and the porosity of the medium may not necessarily be constant. In the light of this fact, Singh et al.[27] investigated the effects of the permeability variation on viscous flow past a vertical porous wall in a porous medium when the permeability varies with time.

Leitao et al.[28] have shown that mass transfer resistance is substantially reduced by intraparticle convection. They performed a mathematical analysis and an experimental study on the separation of two protein molecules in a porous medium. Earlier studies on flow through porous media are mainly based on the use of Darcy's law[29], which gives a linear relationship between the flow velocity and the pressure gradient across the porous medium. Preziosi and Farina[30] analyzed the flow of a Newtonian fluid in a porous medium in the presence of mass exchanges between the constituents. Dash et al.[31] employed the Brinkman equation to model the pathological blood flow when the accumulation of the fatty plaques of cholesterol took place in the lumen of an arterial segment. Acharya et al.[32] discussed the magnetic field effects on the free convection and mass transfer flow through porous media with constant suction and constant heat flux. Kumar et al.[33] studied the unsteady laminar free convection flow of an

electrically conducting fluid through a porous medium along a hot porous plate, where the suction velocity is time-dependent. However, none of these studies considered the oscillatory suction velocity of the fluid under the action of a magnetic field.

Takhar et al.[34] studied the unsteady laminar MHD flow and heat transfer in the stagnation region of an impulsively spinning and translating sphere in the presence of buoyancy forces. The hydromagnetic laminar boundary layer flow and heat transfer in a power law fluid over a stretching surface was investigated by Prasad and Vajravelu[35]. Ganesan and Palani[36] studied a problem of transient free convection MHD flow as well as heat and mass transfer for an incompressible viscous fluid.

Pal et al.[37] investigated the steady MHD flow of an electrically conducting fluid in a slowly varying channel in the presence of a uniform transverse magnetic field. The oscillatory entry flow in a plane channel with pulsating walls was studied by Misra et al.[38]. They discussed the influence of the pulsating motion of the channel walls on the oscillatory entry flow. Misra and Shit[39] developed a numerical method to investigate the influence of an external magnetic field on blood flow in arteries in the normal physiological state. These studies bear the promise of multi-fold applications in hemodynamic.

The motivation of this paper is to study the unsteady hydromagnetic flow as well as the associated heat and mass transfer problem in the case of blood flow through a porous vessel in a pathological state, where the lumen of the vessel segment is turned into porous structure due to the accumulation of fats, cholesterol, and blood clots. The analysis presented here pertains to a situation when the artery is subjected to a time-dependent suction velocity and is under the influence of an externally applied magnetic field. The rationale behind the present study is that the porous material within the lumen of the vessel is a non-homogeneous medium for which the permeability is likely to vary with time. Correspondingly, the suction velocity will also vary with time. These aspects are paid due attention in this study. Moreover, the unsteady oscillatory behaviour of the fluid flow is studied here because of the reason that, due to the unsteady motion of the vessel wall/wall temperature, the flow of the fluid becomes unsteady. In addition, the oscillatory free stream velocity or temperature may also contribute to the unsteadiness of the flow. This important point is also considered in modelling the flow. The problem is solved numerically by an appropriate finite difference method. Considering an illustrative example, the numerical computation is performed in order to estimate the flow, temperature, and mass concentration for various values of Hartmann numbers, Prandtl numbers, radiation parameters, Grashof numbers, and Schmidt numbers. The study has the promise of significant application in electromagnetic therapy, which has gained much popularity in recent years in the treatment of cancer.

2 Flow model and its analysis

Although the modelling of blood flow in arteries may appear to be more intuitive by considering tube flow, it is worthwhile mentioning that the flow in a tube resembles the flow behavior in a channel in many respects. This is the opinion of several previous investigators[40–42]. With this rationale, the present problem is formulated by considering channel flow. Blood is treated here as a viscous incompressible electrically conducting fluid. We study the unsteady hydromagnetic flow of a viscous electrically conducting fluid past an infinite horizontal porous plate through a porous medium having time-dependent permeability. The suction velocity is considered oscillatory. We also incorporate the radiation effect of the heat transfer in the fluid. The permeability of the porous medium is considered to be $K'(t') = K_0(1 + \epsilon \sin(n't'))$ (see Ref. [27]), and the suction velocity is assumed to be $v'(t') = v_0(1 + \epsilon \sin(n't'))$ (see Ref. [43]), where K_0 is the constant permeability of the medium, ϵ ($\ll 1$) is a small positive constant, n' is the frequency of oscillation, and v_0 (> 0) is the scale of the suction velocity. In the Cartesian coordinate system, the x'-axis is assumed to be along the plate in the direction of flow, and

the y'-axis is normal to it. A uniform magnetic field is applied normal to that of the flow (see Fig. 1). In the analysis, it is assumed that the magnetic Reynolds number is much less than unity so that the induced magnetic field is negligible in comparison with the applied magnetic field. Furthermore, all the fluid properties are assumed to be constant except for the influence of density variation with temperature. The basic flow in the medium is entirely due to the buoyancy force caused by the temperature difference between the wall and the inside medium.

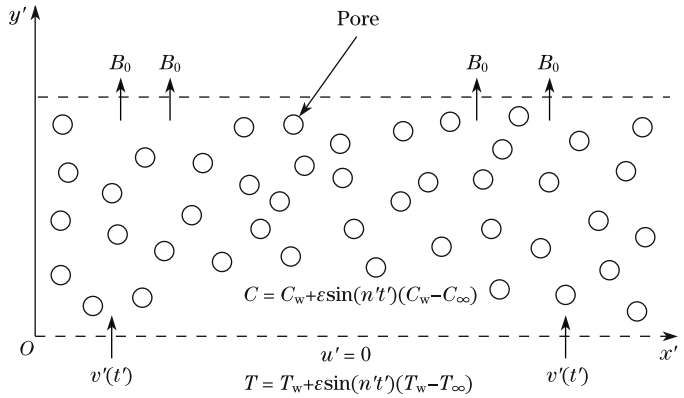

Fig. 1 Physical sketch of problem

The soret effect, also called thermophoresis, is a phenomenon observed when a mixture of different type particles is under the action of a temperature gradient, and the responses of the particles are different, while the Dufour effect refers to the changes in enthalpy due to the diffusion of molecules[17]. At $t' \leqslant 0$, the plate and the fluid are assumed to be at the same temperature, and the concentration of the species is very low so that the Soret and Dufour effects are negligibly small when $t' > 0$, the temperature of the plate is instantaneously raised (or lowered) to the surface temperature ($T_{\rm w}$), and the concentration of species is raised (or lowered) to the concentration of the fluid at the sheet ($C_{\rm w}$).

With all the above-mentioned consideration, taking the usual Boussinesq approximation into account, the equations that govern the motion of the fluid may be listed as

$$\frac{\partial u'}{\partial x'} = 0, \tag{1}$$

$$\frac{\partial u'}{\partial t'} + v'\frac{\partial u'}{\partial y'} = \nu\frac{\partial^2 u'}{\partial y'^2} - \frac{\nu u'}{K'} + g\beta(T - T_\infty) + g\beta^*(C - C_\infty) - \frac{\sigma B_0^2}{\rho}u', \tag{2}$$

$$\frac{\partial T}{\partial t'} + v'\frac{\partial T}{\partial y'} = \frac{k_1}{\rho c_p}\frac{\partial^2 T}{\partial y'^2} - \frac{1}{\rho c_p}\frac{\partial q_{\rm r}}{\partial y'}, \tag{3}$$

$$\frac{\partial C}{\partial t'} + v'\frac{\partial C}{\partial y'} = D\frac{\partial^2 C}{\partial y'^2}. \tag{4}$$

where ν is the kinematic coefficient of viscosity, β is the coefficient of thermal expansion, β^* is the coefficient of thermal expansion with concentration, T is the temperature, T_∞ is the temperature of the ambient fluid, C is the concentration, C_∞ is the concentration of the ambient fluid, B_0 is the strength of the applied magnetic field, c_p is the specific heat at constant pressure, $q_{\rm r}$ is the radiative heat flux, D is the thermal molecular diffusivity, and k_1 is the thermal conductivity. The first term of the left-hand side of each equations of (2)–(4) depicts the transient state. The term $\frac{\nu u'}{K'}$ in the right-hand side of (2) represents the contribution due to the permeability of

the capillary wall. The sum of the terms $g\beta(T - T_\infty)$ and $g\beta^*(C - C_\infty)$ in the same equation represents the body force in terms of temperature and concentration, respectively, while the last term represents the contribution of the external magnetic field. The last term involving $\frac{\partial q_r}{\partial y'}$ in the right-hand side of (3) represents the contribution due to thermal radiation.

The relevant boundary conditions are

$$u' = 0, \quad T = T_w + \epsilon \sin(n't')(T_w - T_\infty), \tag{5}$$

$$C = C_w + \epsilon \sin(n't')(C_w - C_\infty) \quad \text{at} \quad y' = 0, \tag{6}$$

and

$$u' \to 0, \quad T \to T_\infty, \quad C \to C_\infty \quad \text{as} \quad y' \to \infty. \tag{7}$$

By using the Rosseland approximation[44], the relative heat flux is taken in the form

$$q_r = -\frac{4\sigma^*}{3k^*}\frac{\partial T^4}{\partial y'}, \tag{8}$$

where σ^* is the Stefan-Boltzmann costant. We assume that the temperature difference within the fluid is sufficiently small so that T^4 can be expressed as a linear function. Using the Taylor series to expand T^4 about the temperature T_∞ and neglecting the terms of higher powers, we can write

$$T^4 = 4T_\infty^3 T - 3T_\infty^4. \tag{9}$$

Using (8) and (9), we obtain

$$\frac{\partial q_r}{\partial y'} = -\frac{16\sigma^* T_\infty^3}{3k^*}\frac{\partial^2 T}{\partial y'^2}. \tag{10}$$

Let us now introduce the following non-dimensional variables:

$$u = \frac{u'}{v_0}, \tag{11}$$

$$\theta = \frac{T - T_\infty}{T_w - T_\infty}, \tag{12}$$

$$\phi = \frac{C - C_\infty}{C_w - C_\infty}, \tag{13}$$

the following non-dimensional coordinates:

$$y = \frac{y' v_0}{\nu}, \tag{14}$$

$$t = \frac{t' v_0^2}{4\nu}, \tag{15}$$

and the following non-dimensional parameters:

$$K = \frac{K_0 v_0^2}{\nu^2}, \tag{16}$$

$$n = \frac{4n'\nu}{v_0^2}. \tag{17}$$

Substituting (11)–(17) into (2)–(4), we get the following set of equations:

$$\frac{1}{4}\frac{\partial u}{\partial t} + (1+\epsilon\sin(nt))\frac{\partial u}{\partial y} = \frac{\partial^2 u}{\partial y^2} - \frac{u}{K(1+\epsilon\sin(nt))} + Gr\theta + Gm\phi - M^2 u, \tag{18}$$

$$\frac{1}{4}\frac{\partial \theta}{\partial t} + (1+\epsilon\sin(nt))\frac{\partial \theta}{\partial y} = \frac{(1+Nr)}{Pr}\frac{\partial^2 \theta}{\partial y^2}, \tag{19}$$

$$\frac{1}{4}\frac{\partial \phi}{\partial t} + (1+\epsilon\sin(nt))\frac{\partial \phi}{\partial y} = \frac{1}{Sc}\frac{\partial^2 \phi}{\partial y^2}. \tag{20}$$

Also, the boundary conditions (5)–(7) give rise to

$$u = 0, \quad \theta = 1+\epsilon\sin(nt), \quad \phi = 1+\epsilon\sin(nt) \quad \text{at} \quad y = 0, \tag{21}$$

$$u \to 0, \quad \theta \to 0, \quad \phi \to 0 \quad \text{at} \quad y \to \infty. \tag{22}$$

The other non-dimensional parameters that appear in the transformed equations presented above are defined as

$$M = \sqrt{\frac{\sigma\nu}{\rho v_0^2}}B_0, \quad Gr = \frac{g\beta\nu}{v_0^3}(T_{\mathrm{w}} - T_\infty), \quad Gm = \frac{g\beta^*\nu}{v_0^3}(C_{\mathrm{w}} - C_\infty),$$

$$Pr = \frac{\mu c_p}{k_1}, \quad Nr = \frac{16\sigma^* T_\infty^3}{3k^* k_1}, \quad Sc = \frac{\nu}{D}.$$

3 Numerical method

Equations (18)–(20) subjected to the boundary conditions (21) and (22) are solved numerically by a suitable finite difference technique. The central difference scheme is employed to discretize the derivatives with respect to y in (18)–(20) as

$$\frac{\partial F}{\partial y} = \frac{F_{i+1} - F_{i-1}}{2\mathrm{d}y} + O(\mathrm{d}y^2) \tag{23}$$

and

$$\frac{\partial^2 F}{\partial y^2} = \frac{F_{i+1} - 2F_i + F_{i-1}}{\mathrm{d}y^2} + O(\mathrm{d}y^2), \tag{24}$$

in which F stands for u, θ, and ϕ.

The values of u, θ, and ϕ at the mesh point y_i are denoted by u_i, θ_i, and ϕ_i, respectively, and at the jth time-step, the same variables are denoted by u_i^j, θ_i^j, and ϕ_i^j, where

$$y_i = i\mathrm{d}y, \quad i = 1, 2, \cdots, m,$$

$$t_j = j\mathrm{d}t, \quad j = 0, 1, \cdots.$$

Now, applying the Crank-Nicolson formula for (18)–(20), we have

$$A_1 u_{i-1}^{j+1} + B_1 u_i^{j+1} + C_1 u_{i+1}^{j+1} = D_{1i}^j, \tag{25}$$

$$A_2 \theta_{i-1}^{j+1} + B_2 \theta_i^{j+1} + C_2 \theta_{i+1}^{j+1} = D_{2i}^j, \tag{26}$$

$$A_3\phi_{i-1}^{j+1} + B_3\phi_i^{j+1} + C_3\phi_{i+1}^{j+1} = D_{3i}^j \tag{27}$$

with

$$A_1 = -r_1 - r_2, \quad B_1 = 1 + r_2, \quad C_1 = r_1 - r_2,$$

$$D_{1i}^j = u_i^j + r_1(u_{i+1}^j - 2u_i^j + u_{i-1}^j) + 4\mathrm{d}t\Big(- \frac{u_i^j}{Kf} + Gr\ \theta_i^j + Gm\ \phi_i^j - M^2 u_i^j\Big),$$

$$A_2 = -r_1 - \frac{r_2(1+Nr)}{Pr}, \quad B_2 = 1 + 2\frac{r_2(1+Nr)}{Pr}, \quad C_2 = r_1 - \frac{r_2(1+Nr)}{Pr},$$

$$D_{2i}^j = \frac{r_2(1+Nr)}{Pr}(\theta_{i+1}^j - 2\theta_i^j + \theta_{i-1}^j),$$

$$A_3 = -r_1 - \frac{1}{Sc}r_2, \quad B_3 = 1 + \frac{2}{Sc}r_2, \quad C_3 = r_1 - \frac{1}{Sc}r_2,$$

$$D_{3i}^j = \frac{r_2}{Sc}(\phi_{i+1}^j - 2\phi_i^j + \phi_{i-1}^j), \quad r_1 = 2f\frac{\mathrm{d}t}{\mathrm{d}y}, \quad r_2 = \frac{2\mathrm{d}t}{\mathrm{d}y^2}, \quad f = 1 + \epsilon\sin(nt),$$

where $\mathrm{d}y$ and $\mathrm{d}t$ are the mesh sizes along the space and the time directions.

The system of linear equations (25)–(27) is expressed as a tri-diagonal system of equations solved by the Thomas algorithm.

For $j = 0$, the system of (25) may be written as

$$a_i u_{i-1}^1 + b_i u_i^1 + c_i u_{i+1}^1 = d_i^0 \quad \text{for} \quad i = 1, 2, \cdots, m, \tag{28}$$

where

$$a_i = A_1 \quad \text{for} \quad i = 2, 3, \cdots, m, \quad b_i = B_1 \quad \text{for} \quad i = 1, 2, \cdots, m,$$

$$c_i = C_1 \quad \text{for} \quad i = 1, 2, \cdots, m-1, \quad d_i^0 = D_{1i}^0 \quad \text{for} \quad i = 2, 3, \cdots, m-1,$$

$$a_1 = 0, \quad c_m = 0, \quad d_1^0 = D_{11}^0 - A_1 u_0^0, \quad d_m^0 = D_{1m}^0 - C_1 u_m^0.$$

We further write

$$u_i^1 = p_i u_{i+1}^1 + q_i \quad \text{for} \quad i = 1, 2, \cdots, m, \tag{29}$$

$$u_{i-1}^1 = p_{i-1} u_i^1 + q_{i-1} \quad \text{for} \quad i = 1, 2, \cdots, m. \tag{30}$$

For $i = 1$, from (28), we obtain

$$p_1 = -\frac{c_1}{b_1}, \quad q_1 = \frac{d_1^0}{b_1}.$$

Now, eliminating u_{i-1}^1 from (28), we get

$$u_i^1 = -\frac{c_i}{b_i + a_i p_{i-1}} u_{i+1}^1 + \frac{d_i^0 - a_i q_{i-1}}{b_i + a_i p_{i-1}} \quad \text{for} \quad i = 1, 2, \cdots, m, \tag{31}$$

where

$$p_i = -\frac{c_i}{b_i + a_i p_{i-1}}, \quad i = 1, 2, \cdots, m,$$

$$q_i = \frac{d_i^0 - a_i q_{i-1}}{b_i + a_i p_{i-1}}, \quad i = 1, 2, \cdots, m.$$

Let us take

$$u^1_{m+1} = 0. \tag{32}$$

Using (32), from (29), we get

$$u^1_m = q_m. \tag{33}$$

Now, using (29), we can compute u^1_i $(i = m-1, m-2, \cdots, 3, 2, 1)$ in succession.

The same procedure can be adopted for any other value of j, i.e., for any instant of time. Proceeding in a similar manner, we can solve (26) and (27) for temperature and concentration. In the next section, we present the computational results for the major physical quantities, such as the skin-friction (τ), the heat transfer coefficient (Nu), and the mass transfer coefficient (Sb) defined by

$$\tau = \Big(\frac{\partial u}{\partial y}\Big)_{y=0}, \quad Nu = -\Big(\frac{\partial \theta}{\partial y}\Big)_{y=0}, \quad Sb = -\Big(\frac{\partial \phi}{\partial y}\Big)_{y=0}.$$

4 Results and discussion

In order to study the unsteady hydromagnetic heat and mass transfer in the MHD flow of blood through a porous medium inside an artery in a pathological state, with the oscillatory suction velocity, the numerical technique described above was employed to solve the system of equations (18)–(20) subjected to the appropriate boundary conditions (21) and (22).

In order to achieve the numerical solution, it is necessary to assign values of the dimensionless parameters involved in the analysis of the problem under consideration. Computational study has been carried out with an aim to investigate the variation of different quantities of interest involving the following values (see Refs. [45–46]) of the parameters:

$$M^2 = 0.5, 0.8, 1.0, 1.5, 2.0,$$
$$Gr = -25, -13.8, -10, 5, 10, 20,$$
$$Gm = 4, 5, 8, 10, 15, 20,$$
$$Pr = 0.025, 0.1, 0.2, 0.4, 0.7, 0.71, 1.5, 7.0, 10.0,$$
$$Nr = 0.0, 1.0, 1.5, 2.0, 2.5, 4.0, 6.0,$$
$$Sc = 0.1, 0.2, 0.22, 0.15, 0.3, 0.5, 0.9, 1.0, 1.2,$$
$$K = 10.0, \quad n = 2.0.$$

The amplitude parameter ϵ varies between 0.005 to 0.3. The computational work has been performed by $\mathrm{d}y = 0.025$ and $\mathrm{d}t = 0.01$ with 201 grid points. The computed results are presented in Figs. 2–14.

Figures 2–8 focus on the axial velocity u for different values of M^2, Nr, Pr, Sc, Gr, Gm, and ϵ at time $\frac{\pi}{2n}$. Figure 2 reveals that initially the velocity in the axial direction increases upto a certain height of the channel, after which it begins to decrease. One can also note that as the Hartmann number increases, the axial velocity diminishes. However, for low Hartmann numbers, the pick value of the axial velocity is very high. This observation agrees with the theory because with the increase in M, the Lorentz force increases. It is known that the Lorentz force opposes the flow. This implies that if we increase the strength of the magnetic field, the flow of blood will be impeded. It is observed from Fig. 3 that the axial velocity is enhanced with the increase in the radiation. As the value of the radiation parameter reduces, the point at which the axial velocity attains its maximum is shifted nearer and nearer to the lower wall.

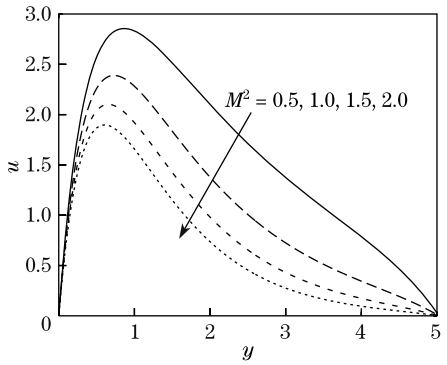

Fig. 2 Velocity distribution for different values of M^2 when $K = 10.0$, $Pr = 0.71$, $Nr = 1.0$, $Sc = 0.22$, $Gr = 10.0$, $Gm = 10.0$, $\epsilon = 0.005$, and $nt = \frac{\pi}{2}$

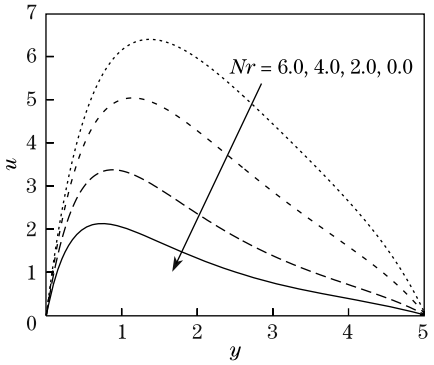

Fig. 3 Velocity distribution for different values of Nr when $K = 10.0$, $Pr = 0.71$, $M^2 = 0.8$, $Sc = 0.22$, $Gr = 10.0$, $Gm = 10.0$, $\epsilon = 0.005$, and $nt = \frac{\pi}{2}$

Figure 4 gives the distribution of the axial velocity for different Prandtl numbers. It is seen from this figure that the axial velocity decreases as the Prandtl number increases and also that with the increase in Prandtl number, the point at which the axial velocity attains its maximum is shifted towards the lower wall. Figure 5 shows that as the thermal molecular diffusivity increases (that is, the Schmidt number decreases), the velocity increases up to a certain height of the channel after which it starts decreasing.

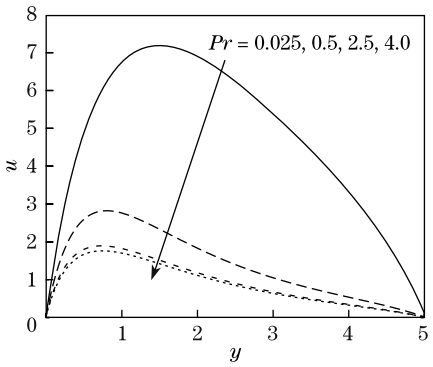

Fig. 4 Velocity distribution for different values of Pr when $K = 10.0$, $M^2 = 0.8$, $Nr = 1.0$, $Sc = 0.22$, $Gr = 10.0$, $Gm = 10.0$, $\epsilon = 0.005$, and $nt = \frac{\pi}{2}$

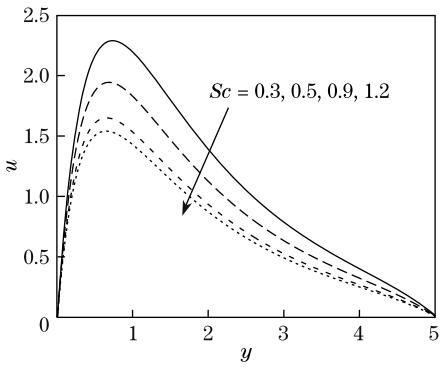

Fig. 5 Velocity distribution for different values of Sc when $K = 10.0$, $Pr = 0.71$, $Nr = 1.0$, $M^2 = 0.8$, $Gr = 10.0$, $Gm = 10.0$, $\epsilon = 0.005$, and $nt = \frac{\pi}{2}$

One can have an idea of the velocity distribution for both cooling of the wall ($Gr > 0$) and heating of the wall ($Gr < 0$) from Fig. 6. It may be noted that in the case of cooling, the velocity decreases as the Grashof number decreases, while in the case of heating, as the Grashof number decreases, the velocity increases. Figure 7 shows that in the case of cooling, the axial velocity decreases as the solute Grashof number decreases. It may be observed from Fig. 8 that the velocity increases with the increase in the value of the amplitude parameter.

Figures 9 and 10 give some characteristic temperature profiles θ for different values of Nr and Pr. It may be observed from these figures that temperature increases with the increase in the radiation parameter/Prandtl number. The plots presented in Fig. 11 indicate that the mass concentration decreases as the Schmidt number increases in the case of cooling of the

channel walls. Figures 12–14 exhibit the distributions of the velocity, temperature, and mass concentration at different instants of time. It is noted that in some time intervals, the velocity, temperature, and mass concentration increase, but in a subsequent interval, they all decrease.

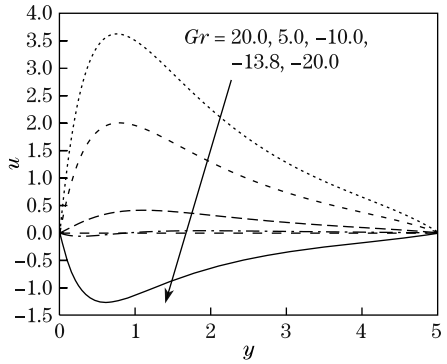

Fig. 6 Velocity distribution for different values of Gr when $K = 10.0$, $Pr = 0.71$, $Nr = 1.0$, $Sc = 0.22$, $M^2 = 0.8$, $Gm = 10.0$, $\epsilon = 0.005$, and $nt = \frac{\pi}{2}$

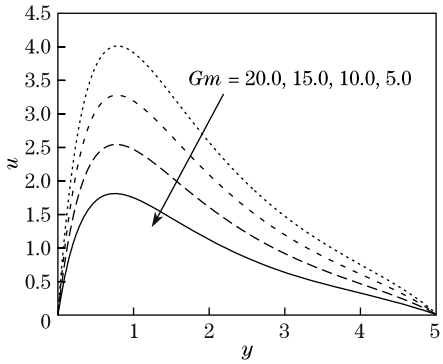

Fig. 7 Velocity distribution for different values of Gm when $K = 10.0$, $Pr = 0.71$, $Nr = 1.0$, $Sc = 0.22$, $Gr = 10.0$, $M^2 = 0.8$, $\epsilon = 0.005$, and $nt = \frac{\pi}{2}$

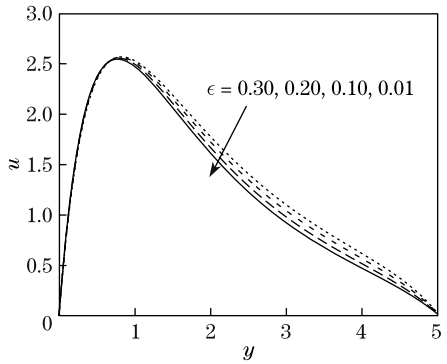

Fig. 8 Velocity distribution for different values of ϵ when $K = 10.0$, $Pr = 0.71$, $Nr = 1.0$, $Sc = 0.22$, $Gr = 10.0$, $Gm = 10.0$, $M^2 = 0.8$, and $nt = \frac{\pi}{2}$

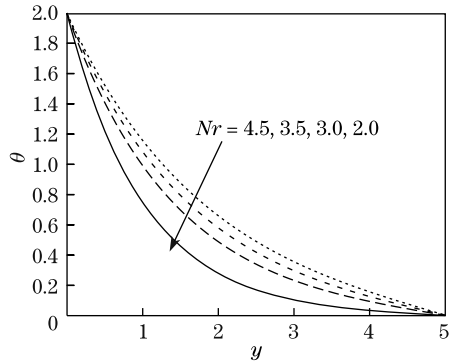

Fig. 9 Temperature distribution for different values of Nr when $M^2 = 0.8$, $Pr = 0.2$, $\epsilon = 0.05$, $Gr = 10.0$, $Gm = 10.0$, $Sc = 0.22$, $K = 10.0$, and $nt = \frac{\pi}{2}$

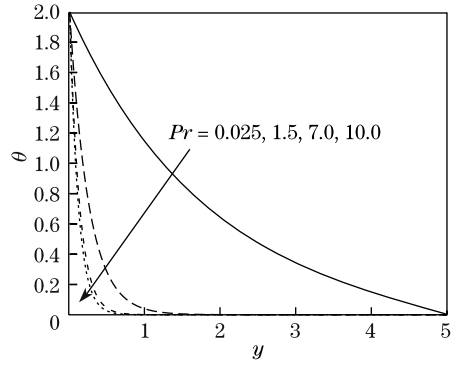

Fig. 10 Temperature distribution for different values of Pr when $M^2 = 0.8$, $Nr = 1.0$, $\epsilon = 0.05$, $Gr = 10.0$, $Gm = 10.0$, $Sc = 0.22$, $K = 10.0$, and $nt = \frac{\pi}{2}$

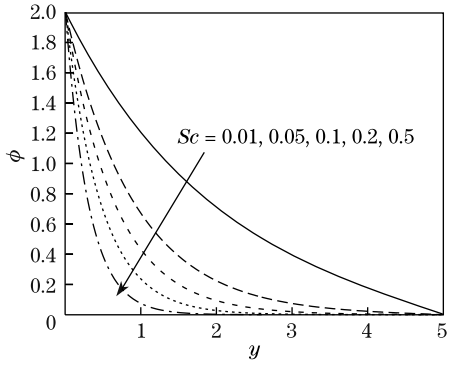

Fig. 11 Variation of concentration profile ϕ for different values of Sc when $M^2 = 0.8$, $Pr = 0.2$, $\epsilon = 0.005$, $Gr = 10.0$, $Gm = 10.0$, $Nr = 1.0$, $K = 10.0$, and $nt = \frac{\pi}{2}$

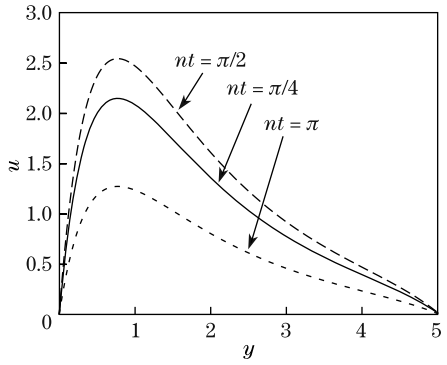

Fig. 12 Velocity field at different instants of time t when $K = 10.0$, $Pr = 0.71$, $Nr = 1.0$, $Sc = 0.22$, $Gr = 10.0$, $Gm = 10.0$, $\epsilon = 0.005$, and $M^2 = 0.8$

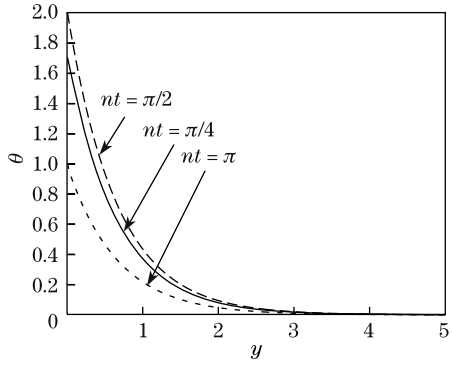

Fig. 13 Variation of temperature profile θ at different instants of time t when $K = 10.0$, $Pr = 0.2$, $Nr = 1.0$, $Sc = 0.22$, $Gr = 10.0$, $Gm = 10.0$, $\epsilon = 0.005$, and $M^2 = 0.8$

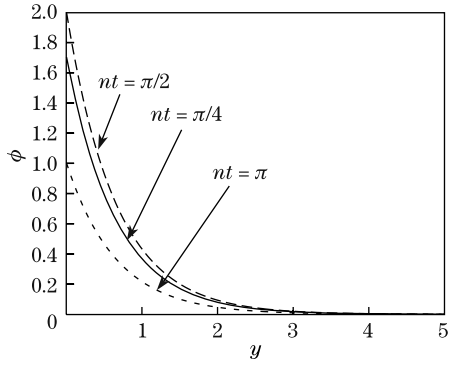

Fig. 14 Variation of concentration profile ϕ at different instants of time t when $K = 10.0$, $Pr = 0.2$, $Nr = 1.0$, $Sc = 0.1$, $Gr = 10.0$, $Gm = 10.0$, $\epsilon = 0.005$, and $M^2 = 0.8$

In Table 1, the numerical values of the skin-friction coefficient for different values of Gr, Gm, M, Sc, Pr, and Nr are presented. With the increases in Gr, Gm, Nr, and Sc, the skin-friction increases, while the increase in M/Pr gives rise to the reduction in the skin-friction. In Table 2, the computed values of Nu for different values of Pr and Nr are displayed. It may be noted that an increase in Pr leads to the increase in the heat transfer, but an increase in Nr brings about a reduction in the heat transfer. Table 3 shows that mass transfer enhances with the increase in the thermal molecular diffusion.

Table 1 Skin-friction coefficients (τ) for cooling of channel walls

Gr	Gm	M^2	Sc	Pr	Nr	τ
10.0	4.0	0.5	0.10	0.4	1.0	8.072 571 75
10.0	8.0	0.5	0.10	0.4	1.0	10.711 718 60
20.0	4.0	0.5	0.10	0.4	1.0	13.503 839 50
10.0	4.0	1.0	0.10	0.4	1.0	7.508 381 37
10.0	4.0	0.5	0.15	0.4	1.0	7.797 169 21
10.0	4.0	0.5	0.10	0.7	1.0	7.197 370 05
10.0	4.0	0.5	0.10	0.4	1.5	8.881 554 60

Table 2 Heat transfer coefficients (Nu) for various Pr and Nr

Pr	Nr	Nu
0.1	1.5	1.700 806 62
0.2	1.5	2.378 273 01
0.1	2.5	1.136 155 13
0.2	2.5	1.613 264 08

Table 3 Mass transfer coefficients (Sb) for different values of Schmidt numbers (Sc)

Sc	0.1	0.2	0.3	0.5	1.0
Sb	2.989 635 47	4.160 237 31	5.018 615 72	6.306 252 48	8.546 872 14

5 Summary and conclusions

The effect of thermal radiation is studied on flow and mass transfer of a viscous, incompressible, and electrically conducting fluid on a studied porous channel with porous boundaries when the suction velocity is of oscillatory nature. The investigation is of significant importance in the study of blood flow through arteries in pathological states, in the situation when the lumen of the artery along with its wall turns porous. The study is quite suitable for the application to the hydrodynamical flow of blood in a coronary artery when it is subjected to the influence of an externally applied magnetic field. The reason is that the porosity of the wall of coronary arteries is quite prominent. The porous matrix in the lumen of the artery is supposed to be formed on account of some particular type of pathology of the artery.

The problem is formulated in terms of a non-linear boundary value problem that has been solved numerically by developing an appropriate finite difference scheme and using the Crank-Nicolson formula.

The results presented here are useful to clinicians, hematologists, and biomedical engineers because they serve as useful estimates, which are capable of throwing some light towards the understanding of genesis of pathological states, like arteriosclerosis as well as the mechanism of gaseous exchanges that take place within tissues and blood vessels. The study may also find applicability in kidney dialysis.

The study has relevance to the physiological flow of blood through coronary arteries whose porosity is quite prominent. The porous matrix formed in the arterial lumen is due to some particular type of pathology of the artery.

The present investigation reveals that blood flow can be controlled by regulating the intensity of the external magnetic field and the temperature of the blood can be controlled by increasing/reducing its thermal conductivity.

Acknowledgements The authors wish to express their deep sense of gratitude to the reviewers for their esteemed comments on the original manuscript. One of the authors (A. SINHA) is grateful to the Council of Scientific and Industrial Research, New Delhi, for the financial support of the investigation.

References

[1] Misra, J. C., Sinha, A., and Shit, G. C. Flow of a biomagnetic viscoelastic fluid: application to estimation of blood flow in arteries during electromagnetic hyperthermia, a therapeutic procedure for cancer treatment. *Appl. Math. Mech. -Engl. Ed.*, **31**(11), 1405–1420 (2010) DOI 10.1007/s10483-010-1371-6

[2] Misra, J. C., Sinha, A., and Shit, G. C. Theoretical analysis of blood flow through an arterial segment having multiple stenoses. *J. Mech. Med. Biol.*, **8**, 265–279 (2008)

[3] Misra, J. C. and Kar, B. K. Momentum integral method for studying flow characteristics of blood through a stenosed vessel. *Biorheology*, **26**, 23–25 (1989)

[4] Misra, J. C., Pal, B., and Gupta, A. S. Hydrodynamic flow of a second-grade fluid in a channel—some applications to physiological systems. *Math. Model. Meth. Appl. Sci.*, **8**, 1323–1342 (1998)

[5] Misra, J. C., Patra, M. K., and Misra, S. C. A non-Newtonian fluid model for blood flow through arteries under the stenotic conditions. *J. Biomech.*, **26**, 1129–1141 (1993)

[6] Misra, J. C. and Roychoudhuri, K. A study on the stability of blood vessels. *Rheol. Acta.*, **21**, 341–346 (1982)

[7] Misra, J. C. and Roychoudhuri, K. Effect of initial stresses on the wave propagation in arteries. *J. Math. Biol.*, **18**, 53–67 (1983)

[8] Misra, J. C. and Shit, G. C. Blood flow through arteries in a pathological state. *Int. J. Eng. Sci.*, **44**, 662–671 (2006)

[9] Misra, J. C. and Shit, G. C. Role of slip velocity in blood flow through stenosed arteries: a non-Newtonian model. *J. Mech. Med. Biol.*, **7**, 337–353 (2007)

[10] Misra, J. C. and Shit, G. C. Biomagnetic viscoelastic fluid flow over a stretching sheet. *Appl. Math. Comput.*, **210**, 350–361 (2009)

[11] Misra, J. C., Shit, G. C., and Rath, H. J. Flow and heat transfer of an MHD viscoelastic fluid in a channel with stretching walls: some applications to hemodynamics. *Comput. Fluids*, **37**, 1–11 (2008)

[12] Misra, J. C. and Singh, S. I. A study on the nonlinear flow of blood through arteries. *Bull. Math. Biol.*, **49**, 257–277 (1987)

[13] Misra, J. C. and Shit, G. C. Flow of a biomagnetic viscoelastic fluid in a channel with stretching walls. *J. Appl. Mech.*, **76**, 061006–061014 (2009)

[14] Misra, J. C., Shit, G. C., Chandra, S., and Kundu, P. K. Electro-osmotic flow of a viscoelastic fluid in a channel: application to physiological fluid mechanics. *Appl. Math. Comput.*, **217**, 7932–7939 (2011)

[15] Misra, J. C. and Chakravarty, S. Dynamic response of arterial walls in vivo. *J. Biomech.*, **15**, 317–324 (1982)

[16] Misra, J. C. and Singh, S. I. Pulse wave velocities in the aorta. *Bull. Math. Biol.*, **46**, 103–114 (1984)

[17] Mortimer, R. G. and Eyring, H. Elementary transition state theory of the Soret and Dufour effects. *Proc. Nat. Acad. Sci.*, **77**, 1728–1731 (1980)

[18] Ramamurthy, G. and Shanker, B. Magnetohydrodynamic effects on blood flow through a porous channel. *Med. Biol. Eng. Comput.*, **32**, 655–659 (1994)

[19] Mustapha, M., Amin, N., Chakravarty, S., and Mandal, P. K. Unsteady magnetohydrodynamic blood flow through irregular multistenosed arteries. *Comput. Biol. Med.*, **39**, 896–906 (2009)

[20] Mekheimer, K. S. Peristaltic flow of blood under effect of magnetic field in a non-uniform channel. *Appl. Math. Comput.*, **153**, 763–777 (2004)

[21] Vardanyan, V. A. Effect of magnetic field on blood flow. *Biofizika*, **18**, 491–496 (1973)

[22] Barnothy, M. F. *Biological Effects of Magnetic Fields*, Plenum Press, New York, 1964–1969 (1964)

[23] Ritman, E. L. and Lerman, A. Role of vasa vasorum in arterial disease: a re-emerging factor. *Current Cardiology Reviews*, **3**, 43–55 (2007)

[24] Khaled, A. R. A. and Vafai, K. The role of porous media in modeling flow and heat transfer in biological tissues. *Int. J. Heat Mass Trans.*, **46**, 4989–5003 (2003)

[25] Jha, B. K. and Prasad, R. Effects of applied magnetic field on transient free convective flow in a vertical channel. *J. Math. Phys. Sci.*, **26**, 1–8 (1992)

[26] Lai, F. C. Coupled heat and mass transfer by mixed convection from a vertical plate in a saturated porous medium. *Int. Comm. Heat Mass Trans.*, **18**, 93–106 (1991)

[27] Singh, A. K., Singh, A. K., and Singh, N. P. Heat and mass transfer in MHD flow of a viscous fluid past a vertical plate under oscillatory suction velocity. *Ind. J. Pure Appl. Math.*, **34**, 429–442 (2003)

[28] Leitao, A., Li, M., and Rodrigues, A. The role of intraparticle convection in protein absorption by liquid chromatography using porous 20 HQ/M articles. *Biochem. Eng. J.*, **11**(2-3), 33–48 (2002)

[29] Darcy, H. R. P. G. *Les Fontaines Publiques de la Voll de Dijan*, Vector Dalmout, Paris (1856)

[30] Preziosi, L. and Farina, A. On Darcy's law for growing porous media. *Int. J. Nonlin. Mech.*, **37**, 485–491 (2002)

[31] Dash, R. K., Mehta, K. N., and Jayaraman, G. Casson fluid flow in a pipe filled with homogeneous porous medium. *Int. J. Eng. Sci.*, **34**, 1146–1156 (1996)

[32] Acharya, M., Dash, G. C., and Singh, L. P. Magnetic field effects on the free convection and mass transfer flow through porous medium with constant suction and constant heat flux. *Ind. J. Pure Appl. Math.*, **31**(1), 1–18 (2000)

[33] Kumar, A., Chand, B., and Kaushik, A. On unsteady oscillatory laminar free convection flow of an electrically conducting fluid through porous medium along a porous hot plate with time dependent suction in the presence of heat source/sink. *J. Acad. Math.*, **24**, 339–354 (2002)

[34] Takhar, H. S., Chamkha, A. J., and Nath, G. Unsteady laminar MHD flow and heat transfer in the stagnation region of an impulsively spinning and translating sphere in the presence of buoyancy forces. *Heat Mass Trans.*, **37**, 397–402 (2001)

[35] Prasad, K. V. and Vajravelu, K. Heat transfer in the MHD flow of a power law fluid over a non-isothermal stretching sheet. *Int. J. Heat Mass Trans.*, **52**, 4956–4965 (2009)

[36] Ganesan, P. and Palani, G. Finite difference analysis of unsteady natural convection MHD flow past an inclined plate with variable surface heat and mass flux. *Int. J. Heat Mass Trans.*, **47**, 4449–4457 (2004)

[37] Pal, B., Misra, J. C., and Gupta, A. S. Steady hydromagnetic flow in a slowly varying channel. *Proc. Natl. Inst. Sci. Ind. Part A*, **66**, 247–262 (1996)

[38] Misra, J. C., Pal, B., Pal, A., and Gupta, A. S. Oscillatory entry flow in a plane channel with pulsating walls. *Int. J. Nonlin. Mech.*, **36**, 731–741 (2001)

[39] Misra, J. C. and Shit, G. C. Effect of magnetic field on blood flow through an artery: a numerical model. *J. Comput. Tech.*, **12**, 3–16 (2007)

[40] Yin, F. and Fung, Y. C. Peristaltic waves in circular cylindrical tubes. *J. Appl. Mech.*, **36**, 679–687 (1969)

[41] Shapiro, A. H., Jaffrin, M. Y., and Weinberg, S. L. Peristaltic pumping with long wavelength at low Reynolds number. *J. Fluid Mech.*, **37**, 799–825 (1969)

[42] Takabatake, S., Ayukawa, K., and Mori, A. Peristaltic pumping in circular cylindrical tubes: a numerical study of fluid transport and its efficiency. *J. Fluid Mech.*, **193**, 267–283 (1988)

[43] Olugu, A. and Amos, E. Modeling pulsatile blood flow within a homogeneous porous bed in the presence of a uniform magnetic field and time dependent suction. *Int. Comm. Heat Mass Trans.*, **34**, 989–995 (2007)

[44] Brewster, M. Q. *Thermal Radiative Transfer Properties*, John Wiley and Sons, New York (1992)

[45] Olugu, A. and Amos, E. Asymptotic approximations for the flow field in a free convective flow of a non-Newtonian fluid past a vertical porous plate. *Int. Comm. Heat Mass Trans.*, **32**, 974–982 (2005)

[46] Chaudhary, R. C. and Jha, A. K. Effect of chemical reactions on MHD micropolar fluid flow past a vertical plate in slip-flow regime. *Appl. Math. Mech. -Engl. Ed.*, **29**(9), 1179–1194 (2008) DOI 10.1007/s10483-008-0907-x